International Journal of Modern Achievement in Science, Engineering and Technology (IJSET)
ISSN 3023-459X
DOI: 10.63053/ijset.69

Assessing the Impact of Reduced Vehicle Volume and Increased Speed on Air Quality in Qom City Using AERMOD

Mohammad Matin Roohbakhsh Panbeh*
Master's student in transportation engineering, Iran University of Science and Technology,Iran

ARTICLE INFO

Keywords:
Air pollution, AERMOD, Traffic, Pollutants, Modeling

ABSTRACT

Urbanization and traffic congestion significantly worsen air pollution, leading to serious health risks. This study examines a scenario involving a 9% reduction in vehicle volume and a 4% increase in vehicle speed on the main roads of Area 6 in Qom City (District 2). The focus is on evaluating the impact of these changes on air quality, specifically concerning pollutants carbon monoxide (CO), nitrogen oxides (NOx), and particulate matter (PM2.5), utilizing AERMOD software for modeling. Data were collected through various methods, including statistical analysis, field sampling within the area, archived records from the Road Administration and the Road Transport Organization of Iran, GPS data for Qom City, and local meteorological information. The results reveal that implementing the proposed traffic management scenario can lead to significant reductions in pollutant levels: CO levels could decrease by approximately 20.19%, NOx by 7.29%, and PM2.5 by 9.00%. These findings underscore the potential of strategic adjustments in traffic patterns to improve urban air quality. The insights gained from this study are valuable for policymakers aiming to tackle environmental challenges in rapidly urbanizing regions, highlighting the importance of effective traffic management in promoting healthier urban environments. Ultimately, enhancing air quality through targeted traffic interventions can improve public health outcomes and contribute to a more sustainable urban future.

Introduction

The increase in urbanization has led to the creation of a dense population in urban areas, along with economic development and the increase in vehicles, which has led to a rise in demand and, as a result, an increase in many challenges regarding mobility and infrastructure (Roohbakhsh Panbeh & Hosseini Gelevardi, 2024). Ambient air pollution and environmental noise significantly impact human health, with air pollution being the leading environmental risk factor in Europe today. In urban areas, road traffic is widely recognized as the primary source of air and noise pollution (European Environment Agency, 2024).

Urban air pollution has become a significant global concern in developed and developing nations. The transportation sector, particularly on-road vehicles, is the primary source of air pollutants in urban areas, posing serious risks to the environment and human health. In cities, on-road vehicles account for up to 80% of air pollution (Grassi & Díaz, 2024). One of the most pressing global challenges is traffic congestion, which significantly impacts national economies. Key factors used to assess its economic effects include travel time, vehicle emissions, and operating costs. The primary causes of traffic congestion are insufficient road capacity, construction issues, traffic incidents, adverse weather conditions, socioeconomic activities, and rapid population growth in urban areas. Additional contributing factors include the rising number of car ownerships, evolving travel patterns, inefficiencies in public transport systems, urban freight transport, goods delivery, parking in outer lanes, and the imbalance between transportation system supply and demand (Moges & Alemu, 2024).

Traffic reduction can be considered one of the solutions to reduce air pollution (European Environment Agency, 2024). For this purpose, this article examines the effects of reducing the volume of vehicles passing through the main transportation routes of Area 6 (District 2 of this Area) of Qom City on air pollution using the AERMOD software. Reducing the volume of traffic can also lead to an increase in the speed of vehicles, and for this reason, in addition to reducing the volume of vehicles, their speed has also been increased. The approximate coordinates of the center of the region are (34.661389011599454,50.834294951069495), and a 9% reduction in the volume of vehicles and a 4% increase in their speed have been applied to the main transportation routes of this region.

Strategies to Reduce Traffic-Related Urban Air Pollution

Three policy strategies have been promoted to mitigate urban air pollution caused by traffic congestion or large traffic volumes. First, local governments could implement traffic control policies to restrict vehicle use and purchases, thereby reducing VEEs. However, vehicle traffic controls negatively impact the logistics sectors and residential demands for daily commuting, and the restriction of car purchases may increase car registration numbers in neighboring cities (Wang & Zhong, 2023).

Second, local governments could invest in road infrastructure, such as extending roads and upgrading fast-pass toll stations, to alleviate traffic congestion and reduce VEEs. However, urban road expansion may alter residential driving behaviors and encourage travel across greater distances, thus further promoting road congestion and air pollution (Wang & Zhong, 2023).

Third, governments could invest in urban road public transport to decrease the use of private motor vehicles, thereby reducing congestion and VEEs. However, due to overestimation of transportation demands, many examples of failed public transit services operated with relatively small passenger volumes after establishment can be found, resulting in relatively high public infrastructure investment losses (Wang & Zhong, 2023).

Air pollution modelling

Air pollution levels are influenced by total emissions, atmospheric transport, and transformation processes, as well as deposition mechanisms. To accurately assess air quality and develop effective emission reduction strategies, all these factors must be taken into account. The complexity of this issue necessitates the use of mathematical modeling tools, commonly referred to as air pollution models (Moussiopoulos, 2013).

Mathematical models are widely employed in environmental science for diverse applications, such as assessing current conditions, conducting statistical analyses, making forecasts, planning, and evaluating scenarios. One of the most intricate challenges involves modeling traffic flow and its associated

atmospheric pollution. This complexity arises from numerous influencing factors, significant variability across daily, weekly, monthly, and yearly scales, and inherent instability in the system (Steinberga et al., 2019).
Various software is used in the field of air pollution modeling, which is suitable for different scales and applications. Figure 1 shows the scales used in air pollution modeling. Also, each union, organization, government, or country uses its own approved specific software. Some of these software are: AERMOD, ADAM, CALPUFF, SLAB, HYROAD, OSPM, ADMS, CALGRlD, EPISODE, and MITRAS (U.S. Environmental Protection Agency | US EPA, 2024; Moussiopoulos, 2013)

Figure 1: Scales used in air pollution modeling

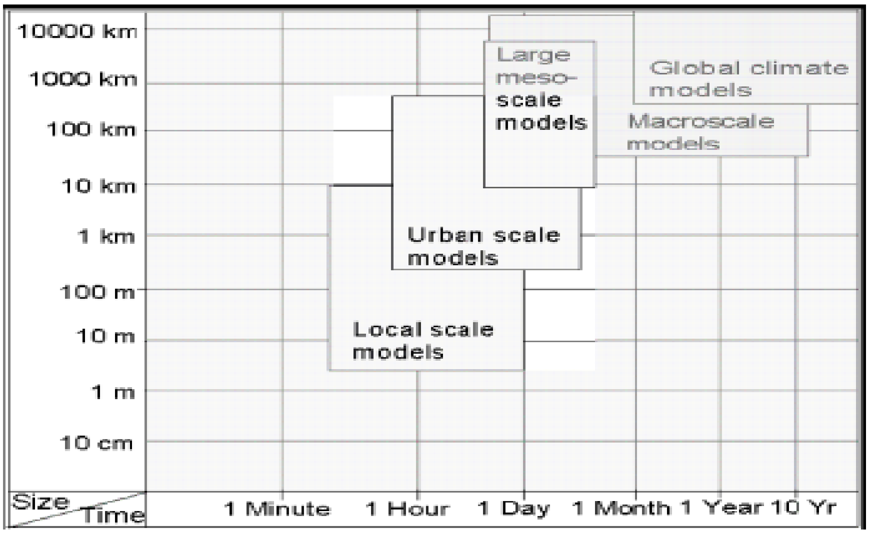

Source: (Moussiopoulos, 2013)

Literature review
Numerous studies have explored air pollution modeling and the application of AERMOD software. Shen et al. (2024) utilized random forest models to estimate traffic counts across European roads, achieving strong 5-fold cross-validation accuracy for most road types. Their research revealed a robust correlation between European and national traffic flow models, improved annual average daily traffic (AADT) estimates, and enhanced Europe-wide air pollution models. This work contributed to the development of higher-resolution urban air pollution maps. Cao (2024) applied machine learning techniques to examine the interplay between traffic volume, air pollution, and meteorological conditions. Using hourly data on traffic volume, NOx, PM2.5, and weather from Oslo, Norway, Cao analyzed six datasets from 2019 to evaluate the predictive accuracy of various models. Pinto et al. (2019) emphasized that outdoor air pollution caused approximately 4.2 million deaths globally in 2016, with road vehicle emissions being the primary source of urban pollution. Their review of over 125 studies identified critical traffic variables necessary for emissions and air quality modeling, stressing the importance of integrating traffic engineering data into emissions models to improve air quality. They also highlighted the need to address uncertainties in traffic data and provided recommendations for different regional applications.
The evaluation of vehicle-induced air pollution in the Brazilian capital using the AERMOD model underscored the effectiveness of mathematical models in environmental impact analysis. By utilizing AERMOD software, the study revealed that CO concentration levels frequently exceeded standard limits, primarily attributed to the high velocity of emission sources. Hourly average concentrations surpassed permissible thresholds, with heavy vehicle emissions identified as the primary contributor (Macêdo & Ramos, 2020). Rowangould (2014) adopted a fast, high-resolution modeling approach with AERMOD to assess regional vehicle emission exposure in Los Angeles, leveraging outputs from travel demand models. The findings highlighted significant diurnal, seasonal, and spatial variations in emission concentrations. In Bahía Blanca, a medium-sized city in Latin America, the AERMOD model was

applied to examine carbon monoxide (CO) and nitrogen oxides (NOx) concentrations between July 2020 and June 2022. The results demonstrated that peak pollutant levels did not directly correspond to traffic patterns, emphasizing the intricate challenges of managing urban air quality (Grassi & Díaz, 2024).
Regarding greenhouse gas emissions from airports, a paper compares AERMOD's performance in describing SO2 concentrations associated with airport sources by comparing model results from the two source options during the summer campaign of the Air Quality Source Apportionment study conducted at the Los Angeles International Airport (Pandey et al., 2024). Pandey et al. (2023) examine the FAA's use of the Aviation Environmental Design Tool (AEDT) and its incorporation of AERMOD to assess airport emissions. They propose a new plume rise formulation for aircraft emissions to address limitations in AERMOD's modeling, which can lead to overestimated ground-level concentrations. The formulation is evaluated using SO2 data from Los Angeles International Airport, demonstrating improved accuracy in predicting concentration behavior (Pandey et al., 2023).
Dos Santos Cerqueira et al. (2018) conducted a study using the AERMOD model to simulate emissions from a power plant. The analysis focused on key pollutants, including VOCs, PM, CO, SO, and NO_x. Findings revealed that pollutant levels emitted from the plant's chimneys posed significant harm to nearby animals and, in particular, plants, as their essential biological processes were disrupted by pollutant absorption. Modeling atmospheric pollutants in thermal power plants using AERMOD software showed that all indicators, except for NO, fall well below standard limits. Nevertheless, these pollutants still threaten the health of local wildlife and vegetation due to bioaccumulation effects (Cerqueira et al., 2018). study by Doost et al. (2023) investigates the dispersion of SO_2 emissions from stacks and flares at a major gas refinery in the Middle East. By measuring SO_2 concentrations at a fixed monitoring station and various distances over a year, the researchers determined pollutant emission coefficients and the contributions of different pollution sources. Utilizing AERMOD, they simulated the SO_2 release pattern and predicted annual pollutant concentrations (Doost et al., 2023). study by Gulia et al. (2015) evaluates urban air quality around a heritage site in Amritsar, India, using the AERMOD model to predict concentrations of nitrogen oxides (NO_x), sulfur dioxide (SO_2), and particulate matter (PM_{10}). The model shows satisfactory performance, and implementing management scenarios could reduce pollutant concentrations by 2.7% for PM_{10}, 9.8% for NO_x, and 7.0% for SO_2 (Gulia et al., 2015).
Comparison between air pollution modeling softwares and selecting the appropriate software for the intended function has always been an important issue. Tartakovsky et al. (2013) conducted a comparative study of the CALPUFF and AERMOD models, finding that AERMOD provided more accurate predictions when validated against measured data. They concluded that employing AERMOD software is unnecessary if accurate digital topographic information is available (Tartakovsky et al., 2013). In India Nath and Dhal (2024) analyze two air quality modeling tools, AERMOD and CALINE4, each offering distinct capabilities for modeling air pollutants from vehicular and other emissions (Nath & Dhal, 2024).

Methods

An effective way to mitigate air pollution is by reducing traffic volume, though this can often lead to increased vehicle speeds. The AERMOD software has been used to assess the combined effects of reduced traffic volume and increased speed on air pollution. The study analyzed the Impacts of a 9% decrease in vehicle volume and a 4% increase in vehicle speed in Area 6 of Qom City (District 2), situated at coordinates (34.661389011599454, 50.834294951069495). This analysis has been conducted on CO, NO_X, and $PM_{2.5}$ pollutants.

Required Data

Data for the analysis were collected Through statistical methods, field sampling within the designated area, archived records from the Road Administration and Road Transport Organization of Iran (Road Administration and Road Transport Organization of Iran, 2024), GPS coordinate of Qom City (Latitude and Longitude Finder on Map Get Coordinates, 2024; Qom, Iran Flood Map: Water Level Elevation Map, 2024), and meteorological data of Qom (Datos Meteorológicos De SYNOPS/BUFR - Predicciones GFS/ECMWF - Meteomanz.com, 2024); Table 1 shows the GPS coordinate of Qom City.

Table 1: GPS coordinate of Qom City

Country: Iran	Country Code: IR-98
Category: Cities	Elevation: 933
Latitude: 34.639999	Longitude: 50.876389
DMS Lat: 34° 38' 23.9964" N	DMS Long: 50° 52' 35.0004" E
Zoom Level: 14	UTM Zone: 39S
UTM Easting: 488,671.11	UTM Northing: 3,833,128.45

Source: (Latitude and Longitude Finder on Map Get Coordinates, 2024; Qom, Iran Flood Map: Water Level Elevation Map, 2024

Roads Data

A portion of the data necessary for modeling in the AERMOD software includes road-related information such as length, width, capacity, traffic volume, and speed limits. Some of this data was collected through sampling and statistical analysis at the study site, while the rest was sourced from the Road Administration and Road Transport Organization of Iran (Road Administration and Road Transport Organization of Iran, 2024). Visual representations of the district's free-flow speed, road capacity, and average traffic volume are provided in Figure 1, Figure 2, and Figure 3, respectively.

Figure 2: The free speed on the roads of the District

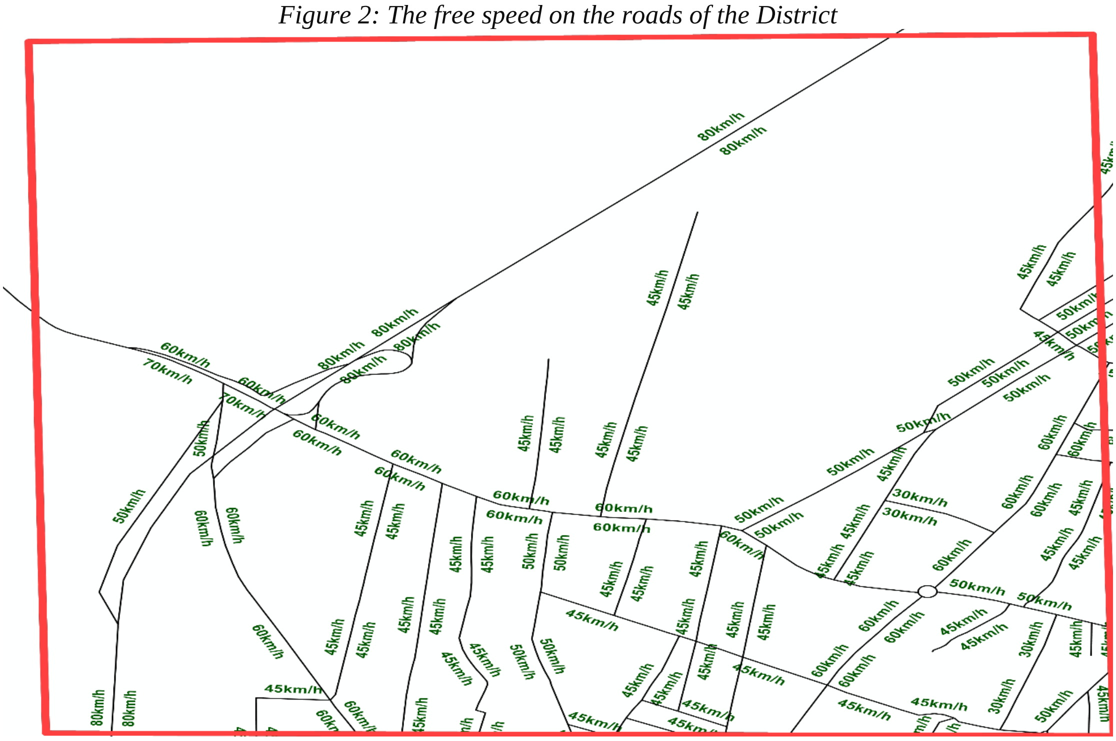

Source: (Road Administration and Road Transport Organization of Iran, 2024)

Figure 3: The capacity of the roads of the District

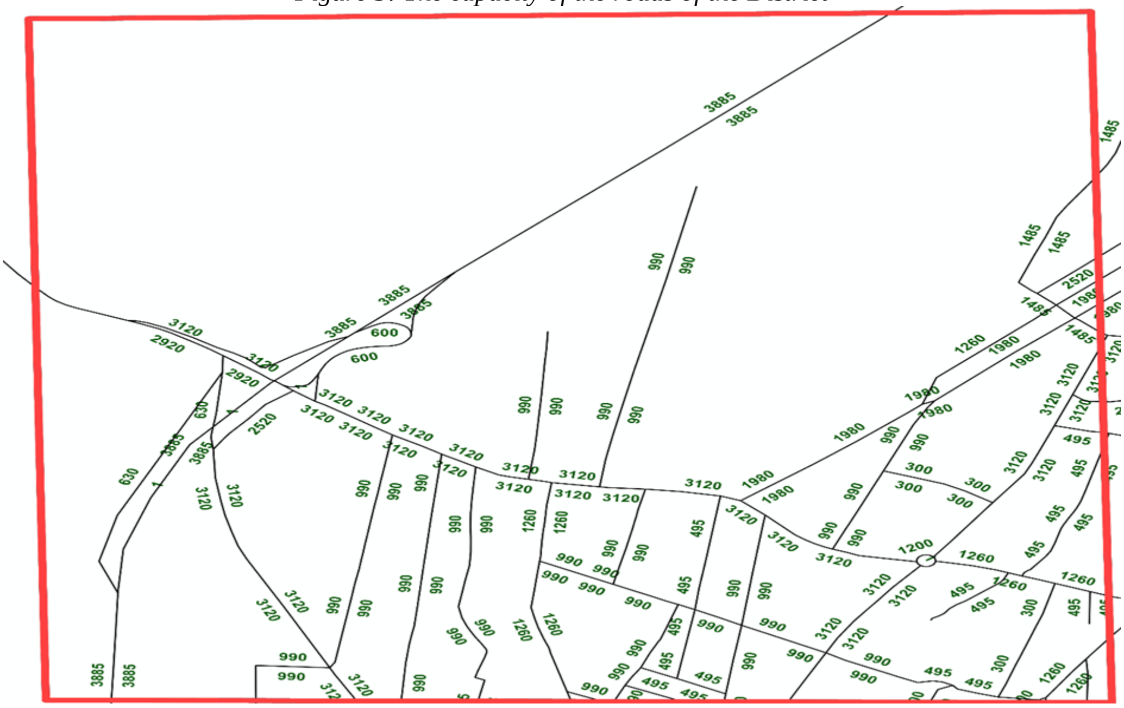

Source: (Road Administration and Road Transport Organization of Iran, 2024)

Figure 4: The average volume passing through the roads of the District

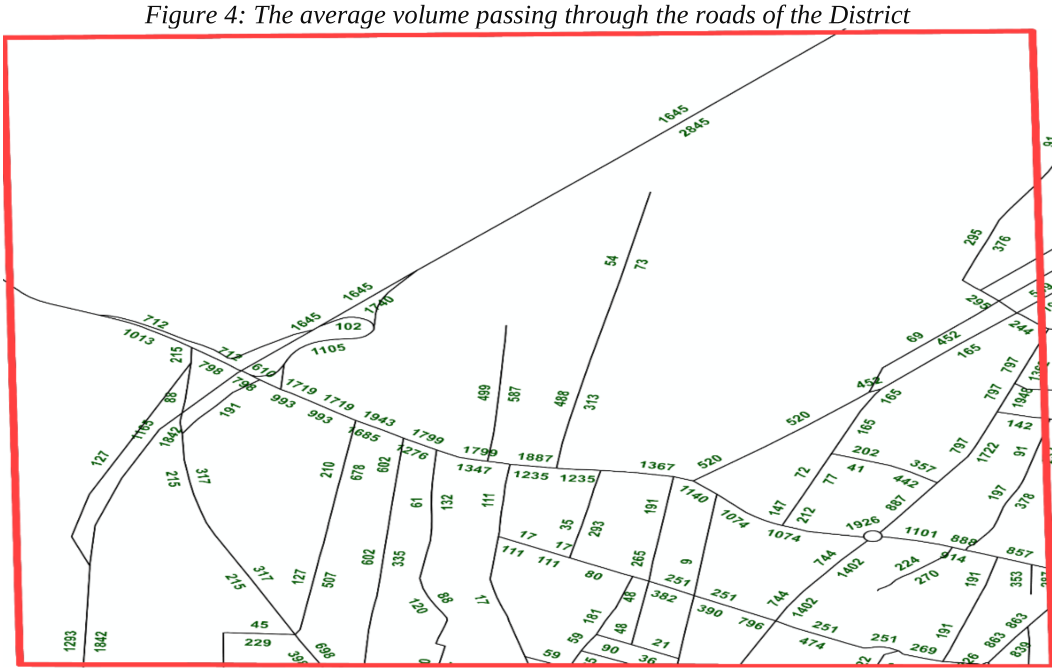

Source: (Road Administration and Road Transport Organization of Iran, 2024)

Because a 4% increase in the free speed of roads for speeds less than 50 km/h results in a speed increase of less than 2 km/h, roads with a free speed greater than or equal to 50 km/h or with high traffic have been selected as selected roads, as shown in Figure 5 of these roads.

Figure 5: Selected roads that are modeled in AERMOD software

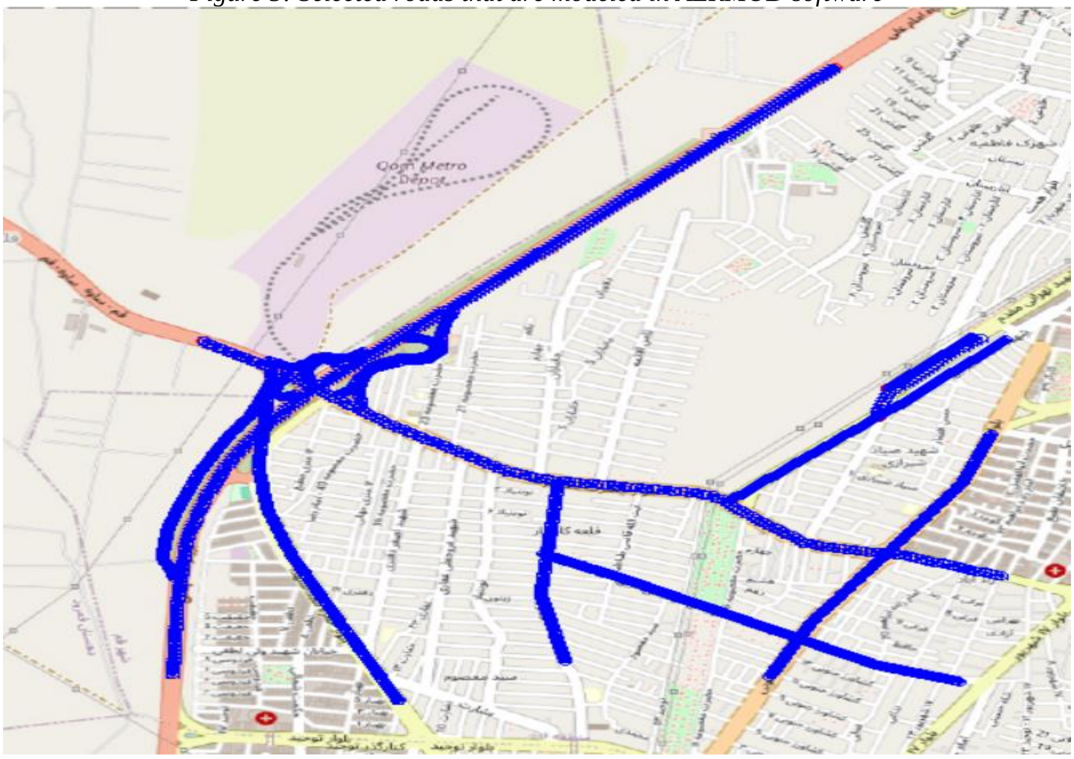

In this study, 18 selected roads have been sampled among the roads in the study area. Table 2 contains data on the route and width of the 18 sampled roads. Some roads are one-way, and some are two-way. For two-way roads, sampling was done in both directions of roads, and the information for each side of these roads has been shown in separate rows in Table 2. If there is no intersection on a road, the volume of vehicles passing through that intersection is constant. For this reason, to draw the roads, as long as there was no intersection and the volume of cars passing was stable, the roads have been drawn sequentially. Similarly, wherever there was an intersection and the volume of vehicles passing changed, the roads have been drawn separately. This way of defining the roads helps to enter more accurate information about the volume and type of vehicles passing through these roads into the AERMOD software and to perform modeling with greater accuracy. Finally, 17 routes have been drawn in the AERMOD software.

Table 2: Sampled roads in the designated district

No.	Road	Number of lane(s)	Width of each lane	Road width
1	Imam Ali Highway to Imam Sadeq Highway	4	3.66	14.64
2	Imam Sadeq Highway to Imam Ali Highway	4	3.66	14.64
3	Imam Ali Highway to Jafariyeh Road	2	3.66	7.32
4	Imam Ali Highway to Hazrat Masoumeh Boulevard	2	3.66	7.32

5	Hazrat Masoumeh Boulevard to Imam Ali Highway	2	3.66	7.32
6	Towards Arak	2	3.66	7.32
7	Hamzeh Seyyed Al-Shohada Boulevard to Hazrat Masoumeh Boulevard	3	3.66	10.98
8	Jafariyeh Road to Seyyed Al-Shohada Boulevard	2	3.66	7.32
9	Seyyed Al-Shohada Boulevard to Tohid Boulevard	3	3.66	10.98
10	Jafariyeh to Hazrat Masoumeh to Imamzadeh Ibrahim	2	3.66	7.32
11	Imamzadeh Ibrahim to Hazrat Masoumeh to Jafariyeh	2	3.66	7.32
12	Keshavarz Boulevard to Kargar Boulevard	2	3.66	7.32
13	Keshavarz Boulevard to Nabuwwat Square	2	3.66	7.32
14	Tehrani Moghadam Boulevard to Hazrat Masoumeh Boulevard	2	3.66	7.32
15	Hazrat Masoumeh Boulevard to Sayyad Shirazi	2	3.66	7.32
16	Hooshangi to Fatemeh Zahra	1	3.66	3.66
17	Hazrat Masoumeh to Fatemeh Zahra	1	3.66	3.66
18	Fatemeh Zahra to Hooshangi	1	3.66	3.66

Meteorological Data

Meteorological information is one of the important information required in modelling with AERMOD software. Table 3 includes meteorological information for Qom City on 5th February 2024, the sampling day, whose data is shown hourly.

Table 3: meteorological information for Qom City

year	month	day	hour	Temp.(ºC)	Rel. h. (%)	SLP(Hpa)	W. sp.(km/h)	Wind dir.	Min.T.(ºC)	Max.T.(ºC)
2024	2	5	1	6.9	42	1019.2	12	246º/SW	2.8	6.9
2024	2	5	2	11.5	30	1014.7	33	266º/W	7	11.8
2024	2	5	3	7.7	43	1016.2	19	240º/SW	7.6	11.5
2024	2	5	4	7.4	43	1015.3	25	245º/SW	7.2	8
2024	2	5	5	8.9	39	1015.3	35	253º/W	6.4	8.9
2024	2	5	6	13.2	28	1012.4	37	271º/W	9.1	13.5

2024	2	5	7	8.7	45	1017.1	26	262º/W	8.6	13.1
2024	2	5	8	6.7	48	1019.1	20	253º/W	6.7	8.7
2024	2	5	9	8.8	40	1021.2	10	252º/W	5.1	8.8
2024	2	5	10	14	26	1017.9	13	260º/W	8.9	14.2
2024	2	5	11	9.2	43	1021	3	272º/W	9.2	14
2024	2	5	12	7.1	50	1021.3	11	271º/W	7.1	9.2
2024	2	5	13	9.9	40	1022	7	252º/W	6	9.9
2024	2	5	14	15.7	21	1017.1	7	308º/NW	10	16
2024	2	5	15	10.6	36	1018.2	4	217º/SW	10.6	15.7
2024	2	5	16	7.7	42	1017.7	7	263º/W	7.7	10.6
2024	2	5	17	11	31	1018.6	6	273º/W	6.5	11
2024	2	5	18	17.3	17	1014.6	10	313º/NW	11.1	17.7
2024	2	5	19	12.3	29	1017	4	253º/W	12.2	17.2
2024	2	5	20	9.2	34	1018.9	6	282º/W	9.2	12.2
2024	2	5	21	12.2	26	1021.7	2	339º/N	7.9	12.2
2024	2	5	22	15.7	21	1019.7	10	73º/E	12.3	15.8
2024	2	5	23	11.6	31	1022.3	4	96º/E	11.6	15.6
2024	2	5	24	8.8	36	1021.8	1	353º/N	8.7	11.5

Source: (Datos Meteorológicos De SYNOPS/BUFR - Predicciones GFS/ECMWF - Meteomanz.com, 2024)

Emission Rate

The emission rate is one of the main variables for modelling in AERMOD software. The formula for obtaining the emission rate can be different according to different sources. Table 4 shows some sources and the formula for obtaining their emission rates.

Table 4: Equations utilized for estimating emission rates

Type of source	Pollutants	Equation	Eq. No.	Description
Burning of crop residue	SO_2, NO_x, PM_{10}	$ER_{(i,c)} = \frac{Q * EF_{(i,c)}}{A * 30 * 24 * 3600}$	(1)	$ER_{(i,c)}$=emission rate ($g/s/m^2$) for i^{th} pollutant from burning of crop residue (c) Q=quantity of crop residue (kg/month) A=area of crop (m^2) $EF_{(i,c)}$=emission factor (g/kg) of i^{th} pollutant emitted from burning of crop residue (c)
Burning of wood in free kitchen	SO_2, NO_x, PM_{10}	$ER_{(i)} = \frac{Q * EF_{(i)}}{24 * 3600}$	(2)	$ER_{(i)}$=emission rate (g/s) for i^{th} pollutant Q=mass of wood burnt (kg/daily) $EF_{(i)}$=emission factor (g/kg) of i^{th} pollutant
Coal-based tandoors	SO_2, NO_x, PM_{10}	$ER_{(i)} = \frac{\sum_{j=1}^{n} Q_{(i,j)} * EF_{(i,j)} * 10^{-3}}{A * 24 * 3600}$	(3)	$ER_{(i)}$=emission rate ($g/s/m^2$) for i^{th} pollutant $Q_{(i,j)}$=mass of coal burnt (kg/day) in n^{th} 'tandoor' $EF_{(i,j)}$=emission factor (g/kg) of i^{th} pollutant

				for n^{th} 'tandoor' A=area (m^2)
Diesel generator	NO_x, PM_{10}	$ER_{(i)} = \frac{\sum_{j=1}^{n} EF_{(i,j)} * W_{(j)}}{A * 3600}$	(4)	$ER_{(i)}$=emission rate ($g/s/m^2$) for i^{th} pollutant $W_{(j)}$=capacity of j^{th} DG set (KW) $EF_{(i,j)}$=emission factor (g/KW-hr) of i^{th} pollutant of j^{th} DG set
Diesel generator	SO_2	$ER_{(SO_2)} = \frac{\sum_{j=1}^{n} Q_{(j)} * D * 2 * S}{A * 3600 * 100}$	(5)	$ER_{(SO2)}$=emission factor SO_2 ($g/s/m^2$) Q=quantity of fuel consumption by j^{th} DG set (l/h) D=density of fuel (kg/m^3) S=sulphur content in fuel (%) n=total number of DG sets in area (A) A=area (m^2)
Re-suspension of road dust	PM_{10}	$EF_{(PM_{10})} = k * (sL)^{0.91} * (W)^{1.02}$	(6)	$EF_{(PM10)}$=emission factor for PM_{10} (g/VKT) k=particle size multiplier (g/VKT), default value of 'k' for PM_{10} is 0.62 g/VKT sL=silt loading for road surface (g/m^2) (0.051 g/m^2) W=average weight of vehicles (in tons) on road

Source: (Gulia et al., 2015)

In this article, Equation 7 is applied to calculate the vehicle emission rate, where $ER_{(i)}$ represents the emissions rate for i^{th} pollutant (g/s), j denotes the type of vehicle (2 W-2S, 2 W-4S, 3 W, 4 W—petrol and diesel driven, bus, truck), $N_{(j,k)}$ indicates the number of vehicles of a particular type 'j' and age of vehicle 'k', $EF_{(i,j,k)}$ stands for the emission factor for pollutant 'i' in the vehicle type 'j' and age 'k' (g/km), and L denotes road length (km). Equation 8 is simplified of Eq. 7 for one type of vehicle ('j') and pollutant(i). 'k' has no effect in Eq. 7. In Eq. 7, N represents the number of vehicles, L denotes the road length (km), and EF stands for the emission factor (g/km). The emission factor values are derived from Euro 4 and Euro 5 standards, with CO emissions set at 2 g/km, NO_X emissions at 0.1 g/km, and $PM_{2.5}$ emissions at 0.005 g/km. The plume height is assumed to match the vehicle exhaust height, fixed at 0.3 meters, while the plume width is equivalent to the road width.

$$\mathrm{ER}_{(i)} = \frac{\sum(j)\sum(k)\, N_{(j,k)} * L * EF_{(i,j,k)}}{3600} \tag{7}$$

$$\text{Emission Rate} = \frac{N * L * EF}{3600} \tag{8}$$

Using sampled data along with data from the Road Administration and Road Transport Organization of Iran, and using Eq. 7, Tables 5 and 6 have been prepared. Table 5 shows the emission rates of the pollutants under analysis in the current conditions of the study area. In contrast, Table 6 depicts the emission rates under the scenario of a 9% decrease in vehicle volume combined with a 4% increase in vehicle speed.

Table 5: Emission rates of the pollutants in the current conditions

Road length(km)	Number of vehicles	CO emissions(g/s)	NOx emissions(g/s)	PM emissions(g/s)	Road width(m)
1.409	4490	3.514672222	0.175733611	0.008786681	14.64
1.72	3286	3.139955556	0.156997778	0.007849889	14.64
0.897	127	0.063288333	0.003164417	0.000158221	7.32
0.442	102	0.025046667	0.001252333	6.26167E-05	7.32
0.53	1105	0.325361111	0.016268056	0.000813403	7.32
0.28	712	0.110755556	0.005537778	0.000276889	7.32

0.131	151	0.0109475	0.000547375	2.73688E-05	7.32
0.156	168	0.01456	0.000728	0.0000364	7.32
2.333	3100	4.017944444	0.200897222	0.010044861	7.32
1.325	612	0.4505	0.022525	0.00112625	10.98
1.14	1842	1.1666	0.05833	0.0029165	7.32
0.52	874	0.252488889	0.012624444	0.000631222	7.32
0.42	617	0.143966667	0.007198333	0.000359917	7.32
0.309	69	0.011845	0.00059225	2.96125E-05	7.32
0.432	165	0.0396	0.00198	0.000099	3.66
0.12	580	0.038666667	0.001933333	9.66667E-05	3.66
0.73	111	0.045016667	0.002250833	0.000112542	3.66

Table 6: Emission rates under the scenario of this paper

Road length(km)	Number of vehicles	CO emissions(g/s)	NOx emissions(g/s)	PM emissions(g/s)	Road width(m)
1.409	4086	3.19843	0.1599215	0.007996075	14.64
1.72	2991	2.858066667	0.142903333	0.007145167	14.64
0.897	116	0.057806667	0.002890333	0.000144517	7.32
0.442	93	0.022836667	0.001141833	5.70917E-05	7.32
0.53	1006	0.296211111	0.014810556	0.000740528	7.32
0.28	648	0.1008	0.00504	0.000252	7.32
0.131	138	0.010005	0.00050025	2.50125E-05	7.32
0.156	153	0.01326	0.000663	0.00003315	7.32
2.333	2821	3.656329444	0.182816472	0.009140824	7.32
1.325	557	0.410013889	0.020500694	0.001025035	10.98
1.14	1677	1.0621	0.053105	0.00265525	7.32
0.52	796	0.229955556	0.011497778	0.000574889	7.32
0.42	562	0.131133333	0.006556667	0.000327833	7.32
0.309	63	0.010815	0.00054075	2.70375E-05	7.32
0.432	151	0.03624	0.001812	0.0000906	3.66
0.12	528	0.0352	0.00176	0.000088	3.66
0.73	102	0.041366667	0.002068333	0.000103417	3.66

Land use

An integral aspect of using AERMOD software is the consideration of land use. It plays a pivotal role in air pollution modeling by significantly affecting the dispersion and transport of pollutants. Additionally, land use data is often employed to estimate emission sources, such as traffic patterns or industrial activities, which are crucial inputs for air quality models. Figure 6 demonstrates the integration of land use data of study place into AERMET.

Figure 6: land use of study place

2 AERMET

AERMET is a meteorological data preprocessor for AERMOD. AERMET processes commercially available or custom on-site met data and creates two files: a surface data file and a profile data file. The tool AERSURFACE can estimate the surface characteristics for input to AERMET (U.S. Environmental Protection Agency | US EPA, 2024). Figure 7 and Figure 8 illustrate the wind rose diagram and the wind class frequency distribution diagram, respectively. Similar to Figure 6, Figure 7 and Figure 8 have been generated using AERMET.

Figure 7: Wind rose diagram

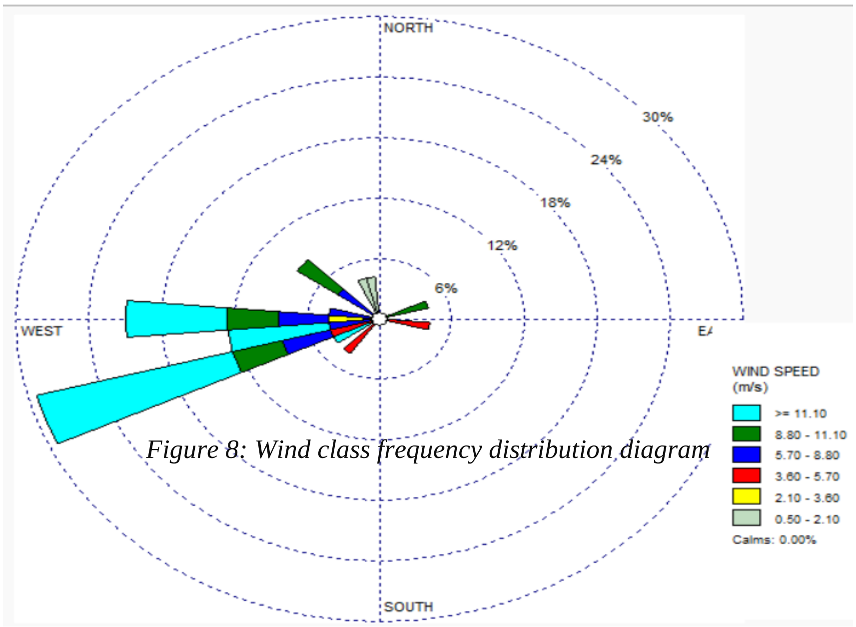

Figure 8: Wind class frequency distribution diagram

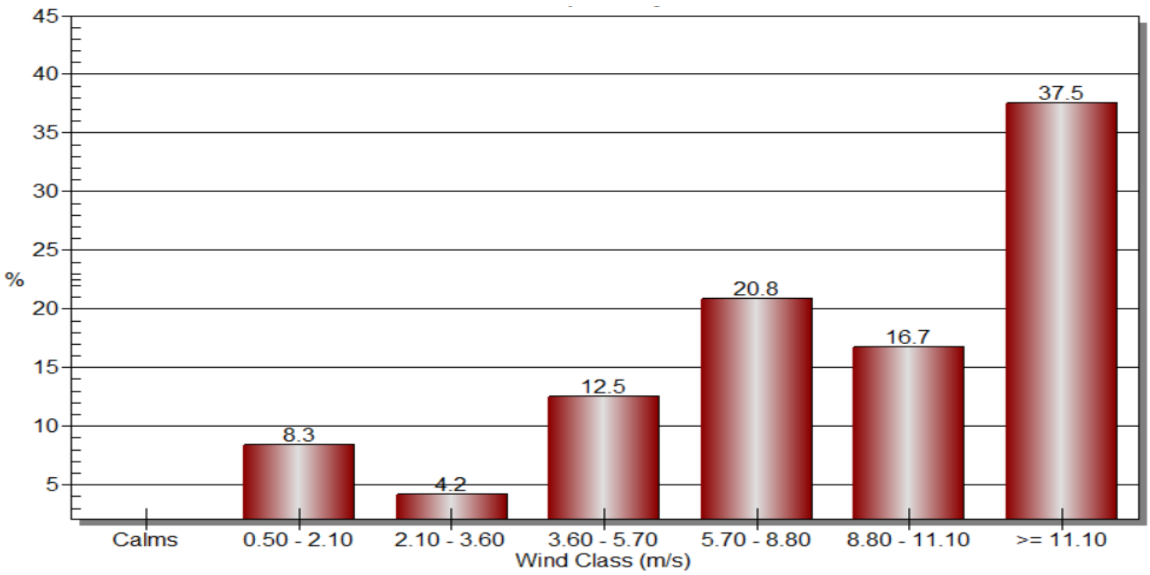

3 Results

To assess the impact of a 9% reduction in vehicle volume alongside a 4% increase in vehicle speed on air pollution, dispersion plots were created to illustrate hourly concentrations of CO, NO_X, and $PM_{2.5}$ pollutants using data gathered on 5th February 2024. Figure 9 illustrates the dispersion plot of hourly CO concentrations under existing conditions, while Figure 10 represents the same under the proposed scenario in this paper. Likewise, Figure 11 highlights the hourly NO_X concentrations for current conditions, with Figure 12 showcasing the results under the proposed scenario. For $PM_{2.5}$, Figure 13 depicts the hourly concentrations under current conditions, whereas Figure 14 presents the concentrations based on the proposed scenario in this paper.

Figure 9: Dispersion plot of hourly CO concentration under existing conditions

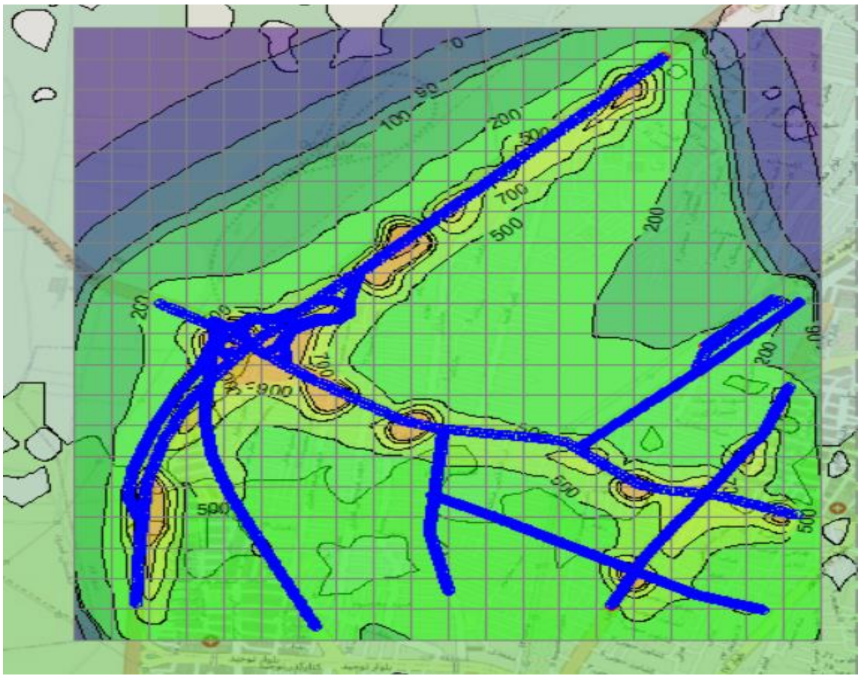

Figure 10: Dispersion plot of hourly CO concentration under the proposed scenario in this paper

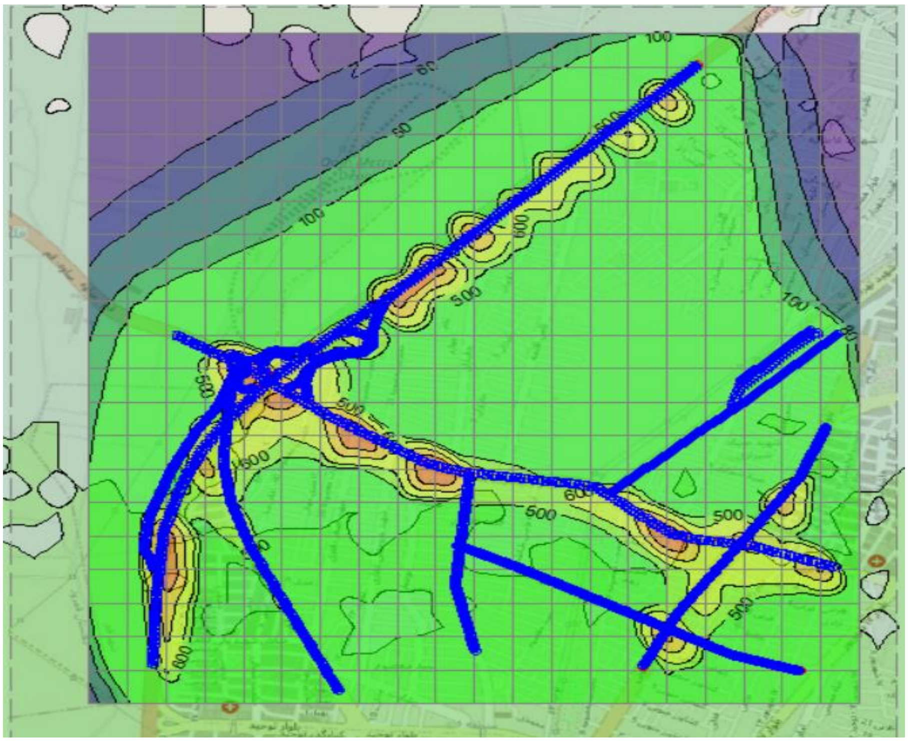

Figure 11: Dispersion plot of hourly NO_X concentration under existing conditions

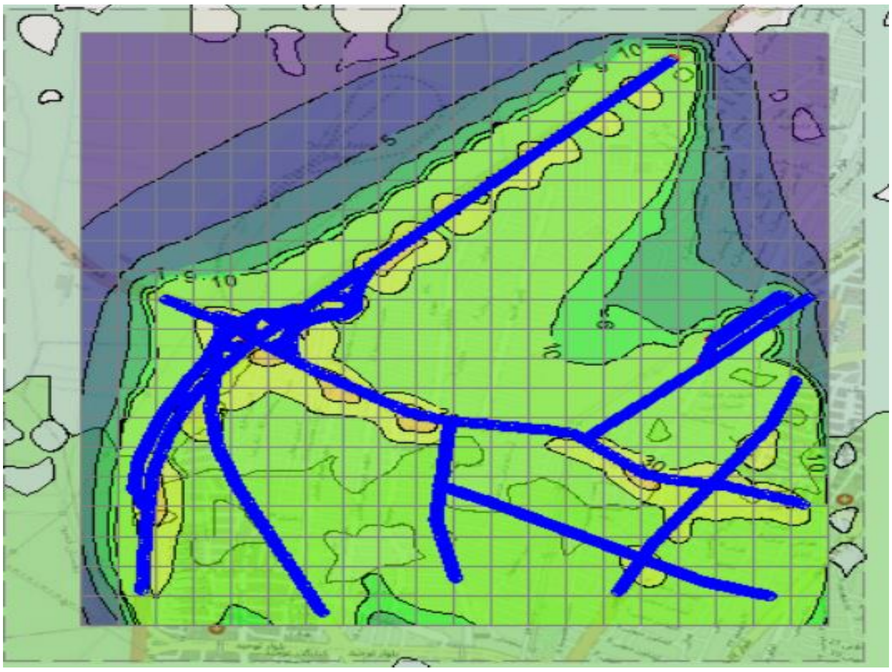

Figure 12: Dispersion plot of hourly NO_X concentration under the proposed scenario in this paper

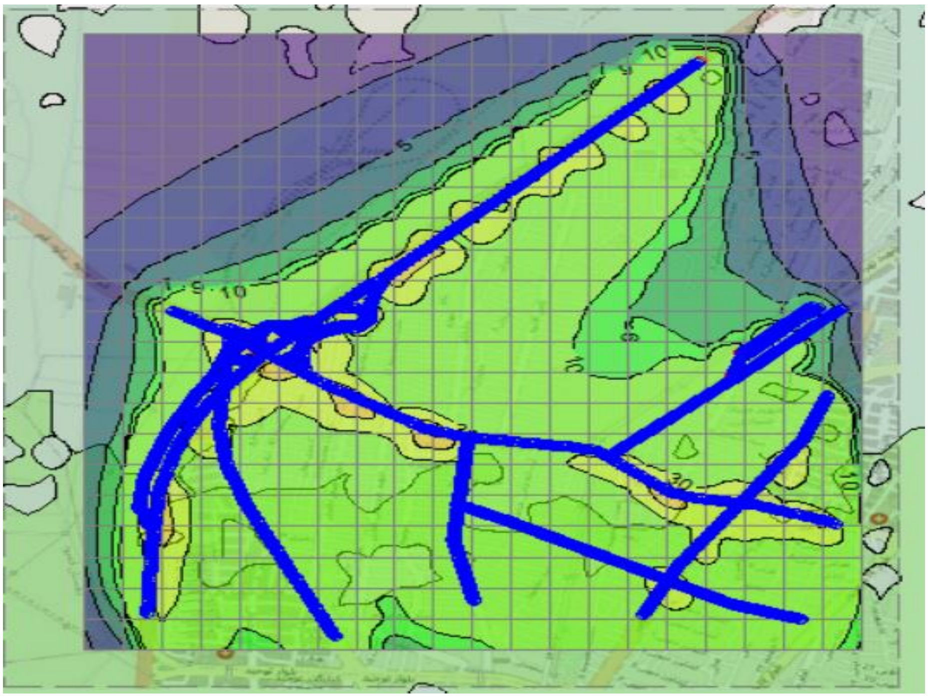

Figure 13: Dispersion plot of hourly $PM_{2.5}$ concentration under existing conditions

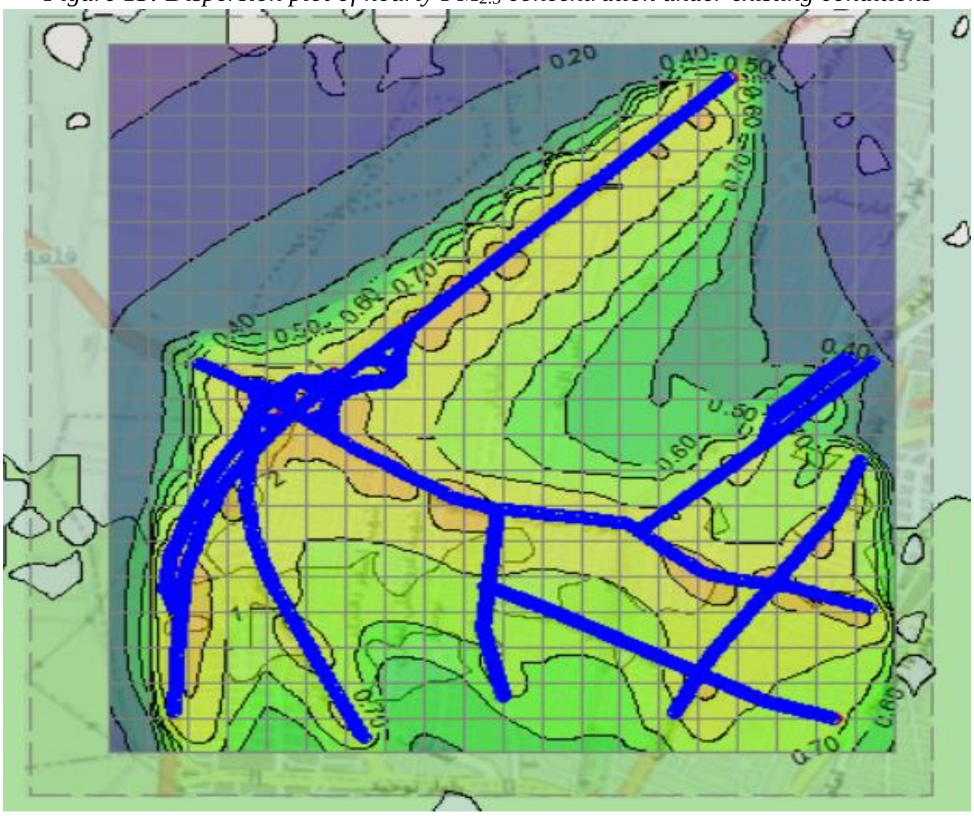

Figure 14: Dispersion plot of hourly $PM_{2.5}$ concentration under the proposed scenario in this paper

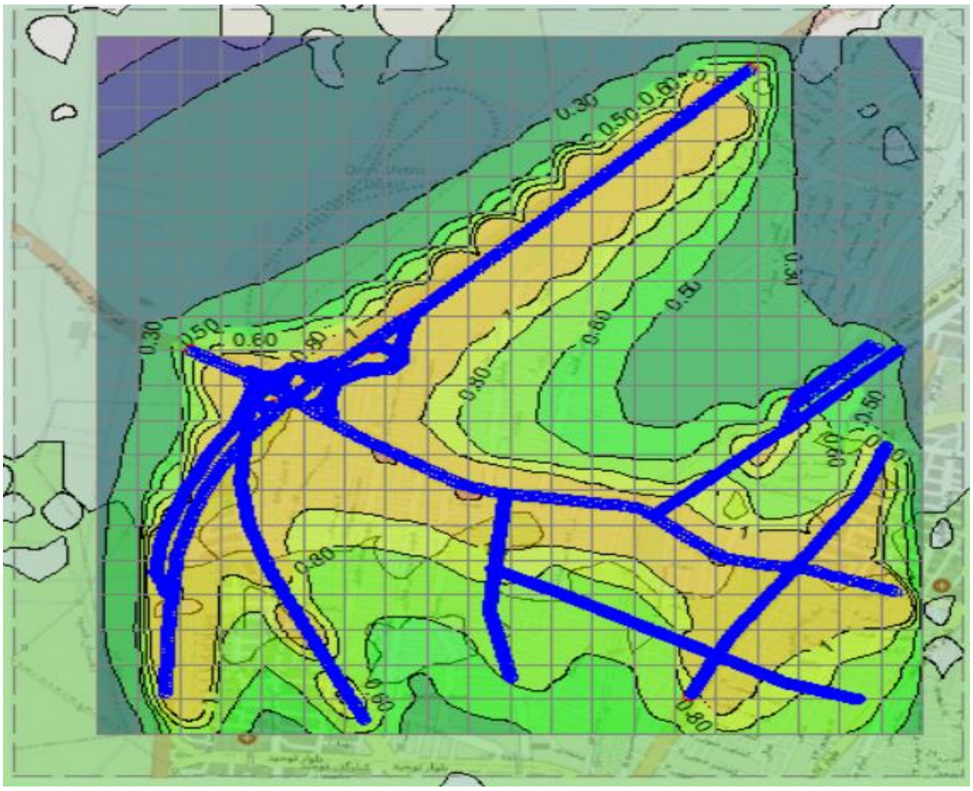

Table 7 shows a summary of the results derived from the dispersion plot of hourly pollutant concentrations for CO, NO_X, and $PM_{2.5}$.

Table 7: Summary of dispersion plot results for CO, NO_X, and $PM_{2.5}$.

Pollutant	**Situation**	**Peak ($\mu g/m^3$)**	**X (m)**	**Y (m)**	**ZELEV (m)**	**ZFLAG (m)**	**ZHILL (m)**	**Difference (%)**
CO	1[1]	1822.77291	485160.72	3836441.35	926.4	1.5	926.4	-20.18609
	2[2]	1454.82637	485160.72	3835622.89	928.4	1.5	928.4	
NOX	1	79.25759	484551.57	3836032.12	927.5	1.5	927.5	-7.288122
	2	73.4812	485160.72	3835622.89	928.4	1.5	928.4	
PM2.5	1	4.03726	485160.72	3835622.89	928.4	1.5	928.4	-8.9962
	2	3.67406	485160.72	3835622.89	928.4	1.5	928.4	

Comparing the summarized results in Table 7 reveals that a 9% reduction in vehicle volume, accompanied by a 4% increase in vehicle speed, leads to a decrease in air pollution levels: approximately 20.19% for CO pollutants, 7.29% for NO_X pollutants, and 9.00% for $PM_{2.5}$ pollutants. Implementing this scenario in the studied area of Qom City could significantly improve air quality.

[1] Situation 1 is the results for the corresponding pollutant tier under current conditions.

[2] Situation 2 is the results for the corresponding pollutant tier when applying a scenario involving a 9% reduction in vehicle volume and a 4% increase in vehicle speed.

Conclusion

Air pollution remains one of the most pressing challenges globally due to its adverse impacts on human health. In urban areas, traffic is the primary contributor to air pollution. This article explores the role of traffic in air pollution and presents strategies to mitigate its effects. By simulating a scenario with a 9% reduction in vehicle volume and a 4% increase in vehicle speed, the study observed a significant decrease in hourly concentrations of CO, NOx, and PM2.5 pollutants. These findings highlight the effectiveness of traffic reduction strategies in combating air pollution in Qom.

The analysis utilized data collected through statistical methods, field sampling within the designated area, archived records from the Road Administration and Road Transport Organization of Iran, GPS coordinates of Qom City, and meteorological data. The AERMOD software was employed to model the dispersion of CO, NOx, and PM2.5 pollutants from traffic sources. Results demonstrated the potential of traffic management strategies to significantly enhance air quality, with reductions of 20.19% in CO, 7.29% in NOx, and 9% in PM2.5.

However, this study was limited to a specific area of Qom City (Area 6, District 2) and a specific time period. Further research is needed to evaluate the long-term impacts and broader applicability of similar traffic management measures. The AERMOD modeling results underscore that even minor adjustments in traffic patterns can lead to substantial reductions in harmful emissions, emphasizing the critical importance of effective urban planning and policy initiatives.

Acknowledgment

Writing this research article would not have been possible without the financial support of the company Kohan Bazar Qarn for the purpose of collecting statistics and sampling. I would also like to express my gratitude to the managers of this company, Mrs. Zahra Heydari Kahkesh and Mr. Mehran Amini Tehrani, who provided me with financial and moral support in this regard.

References

- Cao, C. (2024). How to better predict the effect of urban traffic and weather on air pollution? Norwegian evidence from machine learning approaches. *Journal of Economic Behavior & Organization, 221*, 544–569. https://doi.org/10.1016/j.jebo.2024.03.018
- Cerqueira, J. D. S., De Albuquerque, H. N., & De Assis Salviano De Sousa, F. (2018). Atmospheric pollutants: modeling with Aermod software. *Air Quality Atmosphere & Health, 12*(1), 21–32. https://doi.org/10.1007/s11869-018-0626-9
- *Datos meteorológicos de SYNOPS/BUFR - Predicciones GFS/ECMWF - Meteomanz.com*. (2024). http://www.meteomanz.com/
- Doost, Z. E., Dehghani, S., Samaei, M. R., Arabzadeh, M., Baghapour, M. A., Hashemi, H., Oskoei, V., Mohammadpour, A., & De Marcoc, A. (2023). Dispersion of SO 2 emissions in a gas refinery by AERMOD modeling and human health risk: a case study in the Middle East. *International Journal of Environmental Health Research, 34*(2), 1227–1240. https://doi.org/10.1080/09603123.2023.2165044
- *European Environment Agency*. (2024). https://www.eea.europa.eu/en
- Grassi, Y. S., & Díaz, M. F. (2024). Urban air pollution evaluation in downtown streets of a medium-sized Latin American city using AERMOD dispersion model. *Environmental Monitoring and Assessment, 196*(6). https://doi.org/10.1007/s10661-024-12699-8
- Gulia, S., Shrivastava, A., Nema, A. K., & Khare, M. (2015). Assessment of Urban Air Quality around a Heritage Site Using AERMOD: A Case Study of Amritsar City, India. *Environmental Modeling & Assessment, 20*(6), 599–608. https://doi.org/10.1007/s10666-015-9446-6
- *Latitude and longitude Finder on Map Get Coordinates.* (2024). Lat Long Finder. https://www.latlong.net/
- Macêdo, M. F. M., & Ramos, A. L. D. (2020). Vehicle atmospheric pollution evaluation using AERMOD model at avenue in a Brazilian capital city. *Air Quality Atmosphere & Health, 13*(3), 309–320. https://doi.org/10.1007/s11869-020-00792-z
- Moges, G. T., & Alemu, G. T. (2024). Contribution of congested traffic flow condition to air pollution at intersections in Addis Ababa, Ethiopia. *Heliyon, 10*(17), e36477. https://doi.org/10.1016/j.heliyon.2024.e36477

- Moussiopoulos, N. (2013). *Air quality in cities*. Springer Science & Business Media.
- Nath, A., & Dhal, G. C. (2024). CALINE4 and AERMOD modelling for roadway vehicle-related air pollution: a recent review in India. *Environmental Science and Pollution Research*. https://doi.org/10.1007/s11356-024-34701-z
- Pandey, G., Venkatram, A., & Arunachalam, S. (2023). Accounting for plume rise of aircraft emissions in AERMOD. *Atmospheric Environment, 314*, 120106. https://doi.org/10.1016/j.atmosenv.2023.120106
- Pandey, G., Venkatram, A., & Arunachalam, S. (2024). Modeling the air quality impact of aircraft emissions: is area or volume the appropriate source characterization in AERMOD? *Air Quality Atmosphere & Health, 17*(7), 1425–1434. https://doi.org/10.1007/s11869-024-01517-2
- Pinto, J. A., Kumar, P., Alonso, M. F., Andreão, W. L., Pedruzzi, R., Santos, F. S. D., Moreira, D. M., & De Almeida Albuquerque, T. T. (2019). Traffic data in air quality modeling: A review of key variables, improvements in results, open problems and challenges in current research. *Atmospheric Pollution Research, 11*(3), 454–468. https://doi.org/10.1016/j.apr.2019.11.018
- *Qom, Iran Flood Map: Water Level Elevation map.* (2024). https://www.floodmap.net/?gi=119208
- *Road Administration and Road Transport Organization of Iran.* (2024). https://www.rmto.ir/
- Roohbakhsh Panbeh, M. M., & Hosseini Gelevardi, A. (2024). Investigating the need for urban air mobility in Tehran City. *International Journal of Modern Achievement in Science, Engineering and Technology., 1*(4), 77–97. https://doi.org/10.63053/ijset.49
- Rowangould, G. M. (2014). A new approach for evaluating regional exposure to particulate matter emissions from motor vehicles. *Transportation Research Part D Transport and Environment, 34*, 307–317. https://doi.org/10.1016/j.trd.2014.11.020
- Shen, Y., De Hoogh, K., Schmitz, O., Gulliver, J., Vienneau, D., Vermeulen, R., Hoek, G., & Karssenberg, D. (2024). Europe-wide high-spatial resolution air pollution models are improved by including traffic flow estimates on all roads. *Atmospheric Environment, 335*, 120719. https://doi.org/10.1016/j.atmosenv.2024.120719
- Steinberga, I., Sustere, L., Bikse, J., Bikse, J., Jr, & Kleperis, J. (2019). Traffic induced air pollution modeling: scenario analysis for air quality management in street canyon. *Procedia Computer Science, 149*, 384–389. https://doi.org/10.1016/j.procs.2019.01.152
- Tartakovsky, D., Broday, D. M., & Stern, E. (2013). Evaluation of AERMOD and CALPUFF for predicting ambient concentrations of total suspended particulate matter (TSP) emissions from a quarry in complex terrain. *Environmental Pollution, 179*, 138–145. https://doi.org/10.1016/j.envpol.2013.04.023
- *U.S. Environmental Protection Agency* | US EPA. (2024, January 2). US EPA. https://www.epa.gov/
- Wang, Y., & Zhong, H. (2023). Mitigation strategies for controlling urban particulate pollution from traffic congestion: Road expansion and road public transport. *Journal of Environmental Management, 345*, 118795. https://doi.org/10.1016/j.jenvman.2023.118795